FMCW Implementation of Phase-Attached Radar-Communications (PARC)

Patrick M. McCormick*, Cenk Sahin*, Shannon D. Blunt†, and Justin G. Metcalf‡
*Sensors Directorate, Air Force Research Laboratory, Wright-Patterson Air Force Base, OH
†Department of Electrical Engineering & Computer Science, University of Kansas, Lawrence, KS
‡School of Electrical and Computer Engineering, Advanced Radar Research Center, University of Oklahoma, Norman, OK

***Abstract*—The phase-attached radar-communications (PARC) framework was recently proposed as a means to realize both functions via an FM waveform structure that is amenable to high-power transmitters. This implementation promotes the operation of both functions simultaneously without sacrificing transmission resources (i.e. power, time, frequency) needed for the primary radar mission. Here, the PARC framework is extended to an FM continuous-wave (FMCW) operation which maximizes both data throughput and energy on target. The FMCW PARC waveforms are tested in a open-air environment for ground-based moving target indication (MTI) and the results compared against traditional FMCW stretch processing. As with the original pulsed version of PARC, it is found that the FMCW version introduces Doppler-spread clutter resulting from range sidelobe modulation (RSM), thus necessitating subsequent steps be taken to compensate.**

***Index Terms*—FMCW, stretch processing, radar/communication co-design, range sidelobe modulation**

I. Introduction

As wireless technologies become more pervasive, so does their demand for spectral access. This demand has created tremendous pressure to move away from traditional spectrum allocations, which is particularly problematic for radar operation [1]. In recent years this limitation has spurred research into dynamic spectral access where multiple users coexist within the same band while minimizing interference between the different user functions [2], [3]. In contrast, if multiple RF functions are performed concurrently by the same system (e.g. radar and communications), spectral congestion can also be addressed via co-design of these different functions to more efficiently use a particular band [4]–[14].

An example of dual-function co-design is phase-attached radar-communications (PARC) in which these different modes are combined into a single, frequency modulated (FM) waveform through a summation of two continuous phase structures [9]. The radar phase structure remains unchanged over a coherent processing interval while the communication phase structure is uniquely generated based on the data to be transmitted. The latter is implemented via a continuous phase modulation (CPM) framework that is known to be power efficient and well-contained spectrally [15]. This CPM-based formulation is a general framework that includes the implementations of [7] and [8] as special cases. The PARC framework has been extensively studied from a pulsed perspective [9], [16]–[20], though in such an arrangement the data throughput is inherently limited by the duty cycle.

Here, PARC is extended to a frequency modulated continuous-wave (FMCW) implementation (denoted as FMCW PARC) where it can also be coupled with stretch processing [21]. The "always on" and constant-modulus nature of FMCW PARC allows both data throughput and energy on target to be maximized. Stretch processing is employed so that the radar function is capable of supporting large bandwidths and thus very fine range resolution can be achieved. Consequently, FMCW PARC could be employed in automotive applications to simultaneously support collision avoidance and a vehicle-to-vehicle communication network. It could likewise facilitate the incorporation of a data broadcast component into some forms of synthetic aperture radar (SAR).

The unique data embedded in each FMCW radar sweep results in a waveform-agile transmission mode whereby the same sweep is never repeated. However, over a coherent processing interval (CPI), the unchanging radar phase structure maintains a baseline level of coherence, any deviations from which depend on the parameters of the communication phase structure. This waveform-agile structure does produce a *range sidelobe modulation* (RSM) from sweep to sweep, which subsequently translates into a Doppler smearing of clutter that is not adequately addressed by standard clutter cancellation [17], [19]. However, residual clutter in Doppler due to RSM can be mitigated through appropriate receive filtering [18], [19] or through modification of communication parameters; specifically the data rate or modulation index [9].

Here, the FMCW PARC instantiation is developed and subsequently experimentally tested in an open-air environment for a ground-based moving target indication (MTI) radar mode. The RSM effect is observed for the resulting range-Doppler responses for various modulation indices and data rates. The analog receive chain employs stretch processing to reduce the waveform transmit bandwidth (here 500 MHz) to a much smaller intermediate frequency (IF) bandwidth (here 40 MHz). Leveraging the approach developed in [22] to facilitate waveform-diverse stretch processing, the radar reflections received during each sweep are then range compressed using the appropriate compensation transformation.

II. FMCW PARC with Stretch Processing

The original pulsed PARC structure [9], [16]–[20] is extended for CW operation for a radar function that exhibits a sawtooth wave in instantaneous frequency. When stretch processing is performed in the radar receiver, the mixer output signal is modulated by the PARC communication data. In [22], it was shown that compensation transform (instead of

A portion of this work was supported by the Office of Naval Research under contract #N00014-16-C-2029.
DISTRIBUTION STATEMENT A. Approved for Public Release.

the standard fast Fourier transform (FFT)) can be used to fully compress the data on receive as part of stretch processing for a nonlinear FM transmit scenario (as long as the waveform is relatively chirp-like). Here we leverage this approach for FMCW PARC as well.

A. FMCW PARC Signal Model

The passband FMCW PARC waveform can be defined as

$$s(t;\mathbf{x}) = \cos\left(\psi_{\rm r}(t) + \psi_{\rm c}(t;\mathbf{x})\right), \tag{1}$$

where $\psi_{\rm r}(t)$ is the (passband) phase of the radar component and $\psi_{\rm c}(t;\mathbf{x})$ is the phase of the communication component. The communication phase component is obtained by modulating the $M-$ary symbol sequence $\mathbf{x} = [x_0\, x_1\, x_2\, \cdots]$ with CPM, where $x_n \in \{\pm 1, \pm 3, \cdots, \pm(M-1)\}$ and $m = \log_2 M$ is the number of bits per symbol. The radar phase component is defined as the integral of the radar instantaneous frequency $f_{\rm r}(t)$ as

$$\psi_{\rm r}(t) = 2\pi \int_0^t f_{\rm r}(\tau) d\tau. \tag{2}$$

Here, the shape of $f_{\rm r}(t)$ follows a down-chirped sawtooth wave. For the ith sweep of duration $T_{\rm sw}$ the instantaneous frequency is defined as

$$f_{\rm r}(iT_{\rm sw} \le t < (i+1)T_{\rm sw}) = f_0 - \kappa(t - iT_{\rm sw}), \tag{3}$$

where f_0 is the starting (passband) frequency and $\kappa = B/T_{\rm sw}$ is the chirp rate for B the swept bandwidth.

The communication phase component during the ith sweep is given by[1] [9], [15]

$$\psi_{\rm c}(t;\mathbf{x}) = \pi h \int_0^t \sum_{n=0}^{(i+1)N_{\rm c}-1} x_n\; g(\tau - nT_{\rm c}) d\tau, \tag{4}$$

where $T_{\rm c}$ is the symbol interval, $N_{\rm c} = \frac{T_{\rm sw}}{T_{\rm c}}$ is the number of symbols per sweep, h (a rational number) is the CPM modulation index, and $g(t)$ is the CPM shaping filter (also known as a "frequency pulse" in the CPM literature [15]). The communication symbol rate is thus $B_{\rm c} = \frac{1}{T_{\rm c}}$ symbols/s and the data rate is $mB_{\rm c}$ bits/s. The CPM parameters h, $T_{\rm c}$, $g(t)$, and M uniquely specify the spectrum of the communication phase component $\psi_{\rm c}(t;\mathbf{x})$, and hence the additional receiver bandwidth required to fully capture a given range profile. As such, the CPM parameters are chosen such that the receiver bandwidth does not significantly increase as a result of embedding the communication symbols. Here we focus on full-response CPM [15] with a rectangular shaping filter of duration $T_{\rm c}$ (and amplitude $1/T_{\rm c}$), which is also known as continuous phase frequency shift keying (CPFSK) [23]. In addition, the communication symbol sequence is chosen to be binary, i.e. $x_n = \pm 1$, so that the system performance can be evaluated as a function of h and $T_{\rm c}$.

[1]Here, the CPM modulator does not reset to a state known to the communication receiver in the beginning of each sweep.

The modulation index h is an important system parameter from a CPM perspective as it controls the total phase change due to a communication symbol transmission, which occurs over $T_{\rm c}$. The total phase change due to symbol x_n is therefore $h\pi x_n$, such that the maximum phase change is $\pm h\pi(M-1)$, which becomes $\pm h\pi$ with binary CPM. For pulsed PARC [9], [17], [19] it was shown that h also controls the degree of similarity across the pulse-to-pulse changing radar/communication waveforms. Greater similarity translates to enhanced coherence across the sets of range sidelobes in the CPI, and thus reduced clutter RSM [4], [17]. This relationship between the modulation index value and the severity of RSM is expected to hold for the FMCW PARC instantiation as well.

B. Communication Performance

From a communication perspective, FMCW PARC waveforms have some rather unique properties. First, since radar transmitters are high power devices, the communication receive processing (e.g. channel estimation and synchronization) would likely be performed in the high SNR regime. Second, the transmitted waveforms are partially known at the communication receiver due to the presence of the baseline radar component in (1). By exploiting this structure, channel estimation as well as timing, frequency, and phase offset estimation can be performed in a decision-directed fashion once initial estimates are obtained.

The initial estimates can be obtained in a data-driven fashion by transmitting radar-only sweeps (no communication symbols) during predetermined time intervals, during which the transmitted waveform is completely known at the communication receiver. It is also important to note that the radar signal component possesses some desirable features from an estimation perspective such as high Doppler tolerance.

Third, the received FMCW PARC waveforms have a much larger bandwidth than the communication signal components. As a result, multipath between the radar transmitter and the communication receiver can be resolved at time scales that are much finer than the communication symbol interval. Thus, existing spread spectrum receiver processing approaches (e.g. Rake receiver [24]) should be applicable due to the large ratio of the received signal bandwidth to the communication bandwidth. Determination of the best approaches for communication channel equalization and synchronization for FMCW PARC waveforms is a topic of ongoing research.

Given knowledge of the radar signal component $\psi_{\rm r}(t)$, the communication system parameters, and appropriate channel equalization and synchronization, demodulation at the communication receiver can be performed by multiplying the incident signal $y(t)$ by $\cos(\psi_{\rm r}(t))$ and $-\sin(\psi_{\rm r}(t))$ and lowpass filtering which realizes the complex lowpass equivalent signal

$$\widehat{r}(t;\mathbf{x}) = \sqrt{P_{\rm RX}} \exp\left\{j\psi_{\rm c}(t;\mathbf{x})\right\} + \widehat{n}(t), \tag{5}$$

with real (in-phase) and imaginary (quadrature) components

$$\begin{aligned}\widehat{r}_{\rm I}(t;\mathbf{x}) &= \Phi_{\rm LPF}\left\{\cos\left(\psi_{\rm r}(t)\right)\, y(t)\right\} \\ &= \Phi_{\rm LPF}\left\{\cos\left(\psi_{\rm r}(t)\right)\left(\sqrt{2P_{\rm RX}}\cos\left(\psi_{\rm r}(t) + \psi_{\rm c}(t;\mathbf{x})\right) + n(t)\right)\right\},\end{aligned} \tag{6}$$

$$\begin{aligned}\widehat{r}_{\rm Q}(t;\mathbf{x}) &= \Phi_{\rm LPF}\left\{-\sin\left(\psi_{\rm r}(t)\right)\, y(t)\right\} \\ &= \Phi_{\rm LPF}\left\{-\sin\left(\psi_{\rm r}(t)\right)\left(\sqrt{2P_{\rm RX}}\cos\left(\psi_{\rm r}(t)+\psi_{\rm c}(t;\mathbf{x})\right)+n(t)\right)\right\},\end{aligned} \tag{7}$$

where $\Phi_{\rm LPF}\{\bullet\}$ represents the lowpass filtering operation. Here $P_{\rm RX}$ is the received power, $n(t)$ is a white complex Gaussian noise process with power spectral density N_0, and $\widehat{n}(t)$ is the resulting noise process. The optimal determination of $\mathbf{x}$, which requires maximum likelihood sequence detection, is then achieved by applying the Viterbi algorithm [25] based on a $2v-$state trellis, for v the denominator of h.

Consider a communication receiver located at azimuth angle θ_0 and distance R, and a radar transmitter with peak power $P_{\rm TX}$. The receive power at the communication receiver can be expressed by

$$P_{\rm RX} = \underbrace{\left(\frac{\lambda^2 G_{\rm RX} P_{\rm TX}}{16\pi^2}\right)}_{\mu}\frac{G_{\rm TX}(\theta_0)}{R^2}, \tag{8}$$

where λ is the free-space wavelength, $G_{\rm RX}$ is the receive antenna power gain, and $G_{\rm TX}(\theta_0)$ is the transmit antenna power gain for azimuth angle θ_0. The terms aside from the transmit power gain and distance can be grouped into the constant μ. Therefore, the BER of full-response CPM with a rectangular shaping filter can be approximated as [23]

$$\begin{aligned}&{\rm BER}(h, T_{\rm c}, P_{\rm TX}, \theta_0, R, N_0) \approx \\ &\qquad Q\left(\sqrt{2\mu\frac{T_{\rm c}G_{\rm TX}(\theta_0)P_{\rm TX}}{R^2N_0}\left(1-\frac{\sin 2h\pi}{2h\pi}\right)}\right),\end{aligned} \tag{9}$$

where $Q(x) = \int_x^\infty \frac{1}{\sqrt{2\pi}}\exp\{-t^2/2\}dt$. We refer to the argument of the square root inside the Q function as the *effective communication SNR*, or simply the effective SNR.

It follows that, from a communication performance perspective, it is desirable to increase h. Specifically, it can be shown that for small h the effective SNR decreases approximately by a factor of 4 if h is divided by 2 (a 6 dB loss). Conversely, per (9), increasing $T_{\rm c}$ increases the effective SNR, and hence reduces the BER. However, increasing $T_{\rm c}$ also reduces the symbol rate $B_{\rm c}$. If channel coding is employed, the code blocklength should be chosen as large as possible, as doing so increases the maximum achievable coding rate (expressed as the number of information bits per symbol) that satisfies a given probability of decoding error constraint [26], [27].

Lowering h therefore decreases the maximum achievable coding rate to satisfy a given probability of decoding error constraint [27]. Increasing $T_{\rm c}$ allows for a higher coding rate, while at the same time reducing the code blocklength given that channel coding is performed over a fixed number of sweeps. Thus, whether increasing $T_{\rm c}$ actually improves communication performance depends on the particular implementation.

C. FMCW PARC Range Compression via Compensated Stretch Processing

The FMCW PARC signal can be fully compressed in range using a compensated form of stretch processing recently developed in [22]. The analog portion of the stretch processing system model (see Fig. 1) consists of mixing the received signal with a standard reference $s_{\rm ref}(t)$ down to an intermediate frequency (IF) $f_{\rm IF}$, which is subsequently bandpass filtered (BPF), further mixed down to baseband, and then lowpass filtered (LPF).

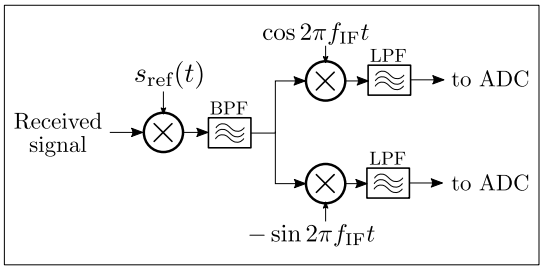

Fig. 1. Analog portion of stretch processing.

Given an IF bandwidth $B_{\rm IF}$ and chirp rate κ, the range swath that can be observed after stretch processing is

$$\Delta r = \frac{cB_{\rm IF}}{2\kappa}, \tag{10}$$

for c the speed of light. The particular location of the range swath is established by time and frequency shifting the reference waveform relative to the transmitted signal so that the mixed product falls inside the IF band of the receiver which is demarcated by $[f_{\rm IF} - \frac{B_{\rm IF}}{2}, f_{\rm IF} + \frac{B_{\rm IF}}{2}]$, where these limits correspond to the near and far edges of the range swath and are denoted as $r_{\rm near}$ and $r_{\rm far}$, respectively, with $\Delta r = r_{\rm far} - r_{\rm near}$.

For standard stretch processing that employs an LFM waveform, reference signal $s_{\rm ref}(t)$ is simply a time and frequency shifted version of the transmitted waveform. Here we set $s_{\rm ref}(t)$ to be a time/frequency shifted version of $\cos(\psi_r(t))$ so that the difference in frequency between $s(t)$ and $s_{\rm ref}(t)$ is minimized for all range delays [22]. Defining the time-shift with respect to an alignment range $r_{\rm a}$ (where $r_{\rm a}$ lies between $r_{\rm near}$ and $r_{\rm far}$), the reference waveform can therefore be expressed as

$$s_{\rm ref}(t) = \cos\left(2\pi f_{\rm a}\cdot(t-\tfrac{2r_{\rm a}}{c}) + \psi_r(t-\tfrac{2r_{\rm a}}{c})\right), \tag{11}$$

where $f_{\rm a}$ is the IF frequency corresponding to range $r_{\rm a}$ and

$$f_{\rm a} = f_{\rm IF} - \tfrac{B_{\rm IF}}{2} + \tfrac{r_{\rm a}-r_{\rm near}}{\Delta r}B_{\rm IF}. \tag{12}$$

The range $r_{\rm a}$ corresponds to the time delay where the sawtooth structure of the reference and received signals are aligned. After compensated stretch processing, this range has the highest signal-to-noise ratio (SNR) and the finest range resolution, and thus $r_{\rm a}$ is the range of highest interest for the radar function.

Because of the additional communication component in waveform $s(t)$, the sampled response (per Fig. 1) is not a tonal structure (i.e. a weighted sum of complex sinusoids) and thus cannot be fully compressed via FFT as is typically applied at the last stage of standard stretch processing. In [22], this effect was addressed (for pulsed, nonlinear FM waveforms) by determining the sampled response at each particular delay and collecting them into the columns of a matrix that forms a compensation transform.

Fig. 2. Field of view for FMCW PARC experimental demonstration for 12.3° transmit and receive antenna beamwidth.

TABLE I
FMCW STRETCH PROCESSING PARAMETERS

Description	Variable	Value
FMCW type	-	sawtooth
FMCW slope	-	down-chirp
Start frequency	f_0	3.85 GHz
Tx bandwidth	B	500 MHz
Sweep time	T_{sw}	500 μs
Chirp rate	κ	1 MHz/μs
Intermediate freq.	f_{IF}	300 MHz
IF bandwidth	B_{IF}	40 MHz
Range swath	Δr	6000 m
Near range	r_{near}	0 m
Far range	r_{far}	6000 m
Alignment range	r_{a}	1050 m
Rx sampling rate	f_{s}	50 MHz
CPI	-	100 ms

For scattering at range r, the complex signal response (in the absence of noise) prior to I/Q sampling can be expressed as

$$p(t,r;\mathbf{x}) = \Phi_{\text{LPF}}\Big\{\Phi_{\text{BPF}}\Big\{s_{\text{ref}}(t)s\big(t-\tfrac{2r}{c};\mathbf{x}\big)\Big\}\exp(-j2\pi f_{\text{IF}}t)\Big\}, \quad (13)$$

where $\Phi_{\text{BPF}}\{\bullet\}$ represents the bandpass filtering operation in Fig. 1, respectively. The response in (13) can then be sampled at the receiver sampling rate (denoted f_{s}) for each range bin, normalized as appropriate, and then applied to the sampled data as the matched filter for that particular range.

Processing the data in this manner accounts for the communication-based signal variations in the transmitted waveform at the cost of a modest increase in computational complexity (due to matrix multiplication instead of the more efficient FFT application). Subsequent Doppler processing across the range compressed sweeps will induce RSM of the clutter due to the sidelobe variations that arise from the changing communication component. Of course, mismatched filter formulations such as considered in [19], [28] could potentially be employed in this FMCW context as well.

III. Open-air Data Collection and Results

The FMCW PARC waveforms were tested in an open-air environment to observe the relationship between the radar performance and the CPM communication parameters of modulation index and symbol rate. Here the evaluated data product is the range-Doppler response that is generated for a traffic intersection in Lawrence, KS that is approximately 1.1 km from the collocated transmitter and receiver located on the roof of Nichols Hall at the University of Kansas. Figure 2 shows the field of view and geometry for this data collect. Two S-band parabolic dish antennas with a half-power beamwidth of 12.3° (illustrated in Figure 2) were used to simultaneously transmit the FMCW PARC waveforms and receive the backscattered response. These waveforms and associated reference signals were generated using a Tektronix AWG70002A arbitrary waveform generator. The backscattered returns (after mixing to IF) were then captured using a Rohde and Schwarz FSW 26 real-time spectrum analyzer.

The instantaneous frequency $f_{\text{r}}(t)$ of the radar component of the transmitted FMCW PARC waveform follows a down-chirped sawtooth with starting and ending frequencies of 3.85 GHz and 3.35 GHz, respectively ($B = 500$ MHz bandwidth), for a $T_{\text{sw}} = 500$ μs sweep time and $\kappa = 1$ MHz/μs chirp rate. The intermediate frequency was set to $f_{\text{IF}} = 300$ MHz with $B_{\text{IF}} = 40$ MHz bandwidth (range swath of $\Delta r = 6000$ m), thus the receiver bandwidth requirements on receive were reduced 12.5 times relative to the transmit bandwidth via stretch processing. The near and far ranges were set to $r_{\text{near}} = 0$ m and $r_{\text{far}} = 6000$ m, respectively. The alignment range was chosen as $r_{\text{a}} = 1050$ m ($f_{\text{a}} = 287$ MHz) so that the maximum SNR and finest range resolution were achieved near the middle of the intersection. The data was sampled at 50 MHz after the mixing and filtering stages. A total of 200 sweeps were captured in the CPI for a total duration of 100 ms. The stretch processing parameters are shown in Table I. To facilitate a fair comparison, all test cases were transmitted back-to-back to illuminate the same approximate scene.

Figure 3 shows the range-Doppler response for two transmission cases: (a) no communications symbols, and thus traditional FMCW stretch processing; and (b) FMCW PARC with modulation index of $h = 1/8$ and 2 Mb/s data rate for a total of 2×10^5 symbols transmitted in the CPI. The radar-only case is processed using standard FFT-based stretch processing while the case with the additional communication function is processed using the compensated transform of [22] formed from (13). The zero-Doppler clutter is removed using a simple projection (since the platform is stationary), and a Hamming window is applied across the pulses to lower the Doppler sidelobes.

The residual clutter due to the RSM effect, which is clearly visible in Figure 3(b), cannot be removed using typical clutter rejection methods[2]. The RSM residue establishes an interference floor across Doppler that could result in false detections or masked targets. While there are methods to reduce the effect of RSM for pulsed emissions (see [6], [16], [18], [19]), this issue is a topic of ongoing research for waveform-diverse stretch processing. Thus for the compensated transform approach con-

[2]Note that coupled range-Doppler processing [18] can also be applied to address the RSM at the cost of increased computational complexity.

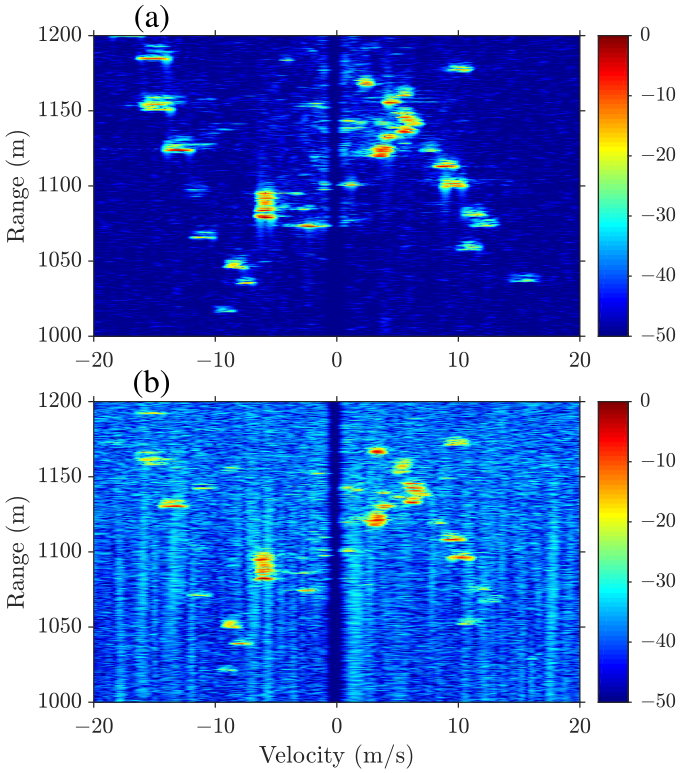

Fig. 3. Range-Doppler response for the cases of (a) radar signal only and (b) PARC with $h = 1/8$ and 2 Mb/s data rate.

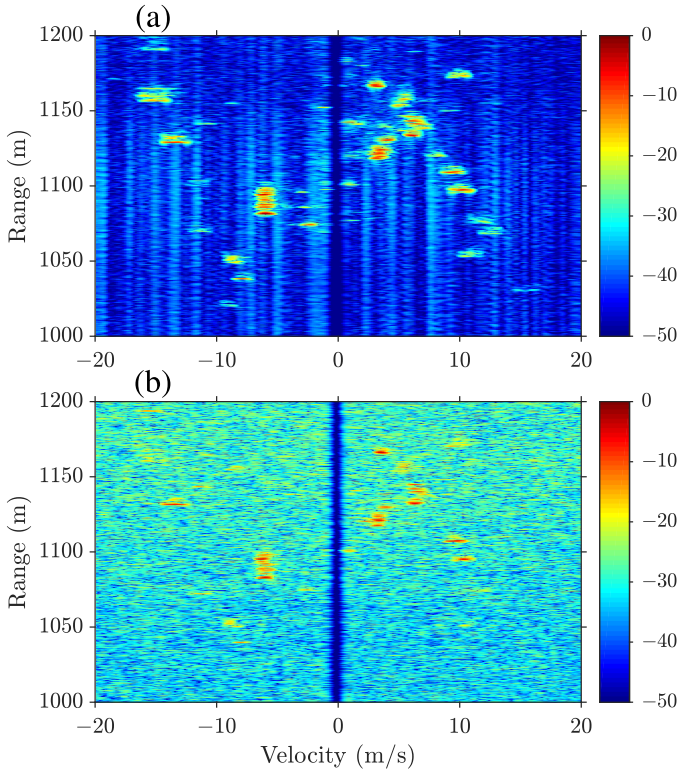

Fig. 4. Range-Doppler response for the cases of (a) PARC with $h = 1/32$ and 2 Mb/s data rate and (b) PARC with $h = 1/2$ and 2 Mb/s data rate.

sidered here, which is effectively a range-dependent matched filter, it is necessary to control the RSM through appropriate parameter selection for the communication function.

Figure 4 shows the range-Doppler responses for modulation indices of (a) $h = 1/32$ and (b) $h = 1/2$ while fixing the data throughput at 2 Mb/s. A decrease in modulation index from $h = 1/8$ in Fig. 3(b) to $h = 1/32$ in Fig. 4(a) corresponds to a smaller phase transition from symbol to symbol, and therefore a smaller deviation from the sawtooth sweep of the radar function resulting in less RSM. However, the effective communication SNR is approximately 12 dB lower for $h = 1/32$ than it is for $h = 1/8$. Thus, the improved radar performance with $h = 1/32$ is achieved at the expense of reduced communication performance in the form of higher BER. Conversely, the $h = 1/2$ case (Fig. 4(b)) increases the deviation from the radar sawtooth wave resulting in significantly greater RSM.

Now fixing the modulation index to $h = 1/32$, Fig. 5 shows the FMCW PARC cases for data throughputs of (a) 500 Kb/s and (b) 8 Mb/s. Compared to the 2 Mb/s case depicted in Fig. 4(a), the increase (or decrease) of the data rate does not significantly effect the RSM relative to the 2 Mb/s case. In fact, the maximum deviation from the radar sawtooth instantaneous frequency is the same for the cases of $h = 1/8$ and 2 Mb/s (Fig. 3(a)) and $h = 1/32$ (8 Mb/s) (Fig. 5(b)), though by inspection the $h = 1/32$ case has a lower RSM power. The increase in symbol rate for a fixed h likewise increases the BER of the transmission scheme, while an increase in modulation index h decreases the BER. Therefore, as previously observed in Fig. 4, the reduced RSM for $h = 1/32$ and data throughput of 8 Mb/s comes at the cost of a higher BER.

The passband content of the FMCW PARC waveform from (1) can be viewed as a convolution between the radar and communication signal components in the frequency domain. Thus, after reference mixing and down-conversion, the resulting signal content is comprised of a superposition of range-dependent, frequency-shifted versions of the communication signal. This spectrum is further compressed using the compensation transform formed from (13). Figure 6 shows the estimated baseband power spectral densities (PSDs) of different communication scenarios normalized to have equal average power. The $h = 1/2$ case occupies the largest bandwidth, and as the modulation index is decreased the PSD becomes better contained. Recall that the $h = 1/8$ (2 Mb/s) and the $h = 1/32$ (8 Mb/s) cases have the same maximum deviation of instantaneous frequency, though the $h = 1/8$ case has a larger spectral breadth than the $h = 1/32$ case. While lowering h does increase the BER (for a fixed symbol rate),it also reduces RSM as seen in Figures 3, 4, and 5.

IV. Conclusions

The PARC framework has been extended for use in an FMCW mode so that higher data rates can be achieved. Due to the high bandwidths involved with the radar component, stretch processing is necessary to reduce the bandwidth of the received signal prior to sampling. However, the use of PARC necessitates replacing the final FFT stage of stretch processing with a compensated transform that was recently developed to

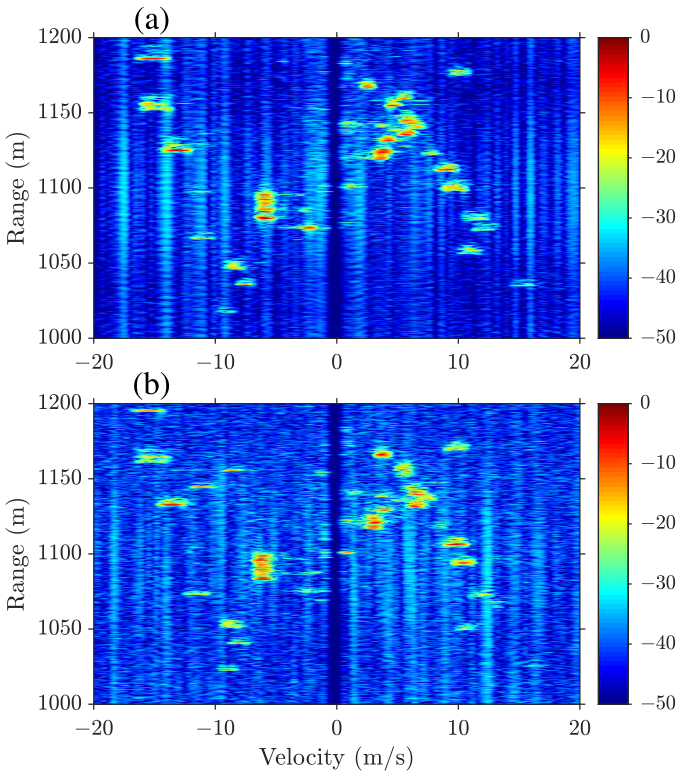

Fig. 5. Range-Doppler response for the cases of (a) PARC with $h = 1/32$ and 500 Kb/s data rate and (b) PARC with $h = 1/32$ and 8 Mb/s data rate.

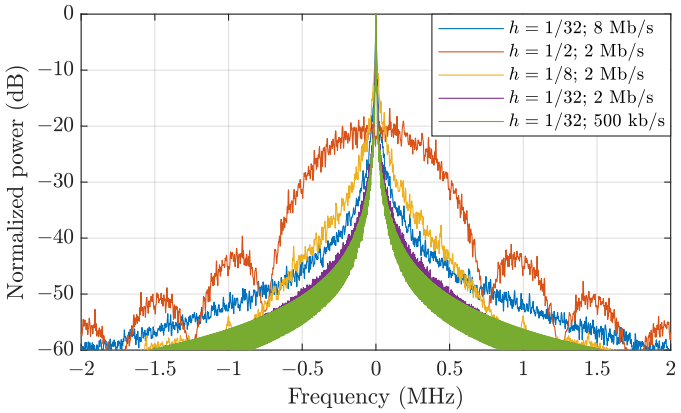

Fig. 6. Estimated power spectra of just the communication component (after reference mixing) for PARC of $h = 1/32$ and 8 Mb/s (blue), $h = 1/2$ and 2 Mb/s (red), $h = 1/8$ and 2 Mb/s (yellow), $h = 1/32$ and 2 Mb/s (purple), and $h = 1/32$ and 500 kb/s (green).

address deviations from the reference signal, which in this case are imposed by incorporating a communication component. As with the pulsed PARC implementation, RSM is found to worsen with increasing symbol rate and modulation index. Based on the power spectral densities after reference mixing, it has been observed that lower modulation indices exhibit better spectral containment which, in this context corresponds to less RSM degradation.

References

[1] H. Griffiths, L. Cohen, S. Watts, E. Mokole, C. Baker, M. Wicks, and S. Blunt, "Radar spectrum engineering and management: technical and regulatory issues," *Proc. IEEE*, vol. 103, no. 1, 2015.

[2] Q. Zhao and B.M. Sadler, "A survey of dynamic spectrum access," *IEEE Signal Process. Mag.*, vol. 24, no. 3, pp. 79–89, May 2007.

[3] D.B. Rawat, M. Song, and S. Shetty, *Dynamic Spectrum Access for Wireless Networks*.Switzerland: Springer International Publishing, 2015.

[4] S.D. Blunt and E.S. Perrins, eds., *Radar & Communication Spectrum Sharing*. London, UK: IET, 2018.

[5] C. Sturm, T. Zwick, and W. Wiesbeck, "An OFDM system concept for joint radar and communications operations," *IEEE Vehicular Tech. Conf.*, Apr. 2009.

[6] S.D. Blunt, M.R. Cook, and J. Stiles, "Embedding information into radar emissions via waveform implementation," *Intl. Waveform Diversity and Design Conf.*, Aug. 2010.

[7] X. Chen, X. Wang, S. Xu, and J. Zhang, "A novel radar waveform compatible with communication," *Intl. Conf. on Comp. Problem-Solving*, Oct. 2011.

[8] M. Nowak, M. Wicks, Z. Zhang, and Z. Wu, "Co-designed radar-communication using linear frequency modulation waveform," *IEEE Aerosp. Electron. Syst. Mag.*, vol. 31, no. 10, Oct. 2016.

[9] C. Sahin, J. Jakabosky, P.M. McCormick, J.G. Metcalf, and S.D. Blunt, "A novel approach for embedding communication symbols into physical radar waveforms," *IEEE Radar Conf.*, May 2017.

[10] B. Ravenscroft, P.M. McCormick, S.D. Blunt, J. Jakabosky, and J.G. Metcalf, "Tandem-hopped OFDM communications in spectral gaps of FM noise radar," *IEEE Radar Conf.*, May 2017.

[11] P.M. McCormick, S.D. Blunt, and J.G. Metcalf, "Simultaneous radar and communications emission from a common aperture, part I: theory," *IEEE Radar Conf.*, May 2017.

[12] N.A. O'Donoughue, "Analysis of dual-transmit beams," *IEEE Radar Conf.*, May 2017.

[13] P.M. McCormick, C. Sahin, S.D. Blunt, and J.G. Metcalf, "Physical waveform optimization for multiple-beam multifunction digital arrays," *The Asilomar Conf. on Signals, Systems, and Computers*, Oct. 2018.

[14] C. Sahin, P.M. McCormick, J.G. Metcalf, and S.D. Blunt, "Power-efficient multi-beam phase-attached radar/communications," *IEEE Radar Conf.*, Apr. 2019.

[15] J.B. Anderson, T. Aulin, and C.E. Sundberg, *Digital Phase Modulation*. New York, NY: Springer US Publishing, 1986.

[16] C. Sahin, P.M. McCormick, and B. Ravenscroft, "Embedding communications into radar emissions by transmit waveform diversity," in *Radar & Communication Spectrum Sharing*, S.D. Blunt and E.S. Perrins, eds. IET, 2018.

[17] C. Sahin, J.G. Metcalf, and S.D. Blunt, "Characterization of range sidelobe modulation arising from radar-embedded communications," *Intl. Conf. on Radar Systems*, Oct. 2017.

[18] C. Sahin, J.G. Metcalf, and B. Himed, "Reduced complexity maximum SINR receiver processing for transmit-encoded radar-embedded communications," *IEEE Radar Conf.*, Apr. 2018.

[19] C. Sahin, J.G. Metcalf, and S.D. Blunt, "Filter design to address range sidelobe modulation in transmit-encoded radar-embedded communications," *IEEE Radar Conf.*, May 2017.

[20] C. Sahin, J.G. Metcalf, A. Kordik, T. Kendo, and T. Corigliano, "Experimental validation of phase-attached radar/communications: Radar performance," *Intl. Conf. on Radar*, Aug. 2018.

[21] W.L. Melvin and J.A. Scheer, *Principles of Modern Radar: Advanced Techniques*. Rayleigh, NC: SciTech Publishing, 2013.

[22] D.M. Hemmingsen, P.M. McCormick, S.D. Blunt, C. Allen, A. Martone, K. Sherbondy, and D. Wikner, "Waveform-diverse stretch processing," *IEEE Radar Conf.*, Apr. 2018.

[23] J.G. Proakis, *Digital Communications*. New York, NY: McGraw-Hill, 2008.

[24] A.F. Molisch, *Wireless Communications*. West Sussex, UK: John Wiley & Sons Ltd., 2011.

[25] A. Viterbi, "Error bounds for convolutional codes and an asymptotically optimum decoding algorithm," *IEEE Trans. Inf. Theory*, vol. 13, no. 2, 1967.

[26] Y. Polyanskiy, H. Poor, and S. Verdu, "Channel coding rate in the finite blocklength regime," *IEEE Trans. Inf. Theory*, vol. 56, no. 5, 2010.

[27] C. Sahin and E. Perrins, "On the symmetric information rate of CPM in the finite blocklength regime," *IEEE Military Comm. Conf.*, Oct. 2015.

[28] L. Harnett, D. Hemmingsen, P.M. McCormick, S.D. Blunt, C. Allen, A. Martone, K. Sherbondy, and D. Wikner, "Optimal and adaptive mismatch filtering for stretch processing," *IEEE Radar Conf.*, Apr. 2018.